JOURNAL OF MATERIALS SCIENCE 2 (1967) 529–537

Scaling and Intergranular Oxidation of an Fe/48 wt % Ni Alloy in Carbon Dioxide at 700 to 1000°C

I. A. MENZIES, W. J. TOMLINSON*
Corrosion Laboratories, Department of Chemical Engineering, University of Manchester Institute of Science and Technology, Manchester 1, UK

Received 25 May 1967, and in revised form 28 July

The oxidation of Nilo 48 has been studied using thermogravimetric, metallographic, and electron probe microanalysis techniques at 700 to 1000° C. After a short period of ill-defined oxidation, the parabolic law was obeyed throughout the exposure period, which varied from ~1050 h at 713° C to 50 h at 1000° C. The activation energy for the oxidation reaction was 48 ± 6 kcal/mole. Examination of the external scale indicated that this was single phase and, at 1000° C, its composition corresponded to $Ni_xFe_{3-x}O_4$, where $x \leqslant 0.4$. There were also intergranular oxidation and nickel enrichment of the alloy underlying the external scale. After oxidation for only 10 min at 1000° C, the nickel-enriched alloy zone contained 65 wt % Ni. The manganese concentration in the scale was similar to that in the alloy. The results are discussed and compared with those of other workers and it is concluded that the rate-controlling process is the diffusion of iron through the $Ni_xFe_{3-x}O_4$ lattice.

1. Introduction

Fe/Ni alloys are important engineering materials because of their special thermal expansion and magnetic properties, and they are of interest in a wide range of industrial applications including glass-to-metal seals. The Fe/Ni system is almost ideal, inasmuch as Raoult's law is obeyed, and the alloys form a continuous series of substitutional solid solutions. Furthermore, under oxidising conditions, where both metals can oxidise, solid-state reactions can occur between the oxides of the metals.

The oxidation of Fe/Ni alloys in air and oxygen has been studied extensively and these investigations have recently been reviewed [1,2]. Much less is known concerning the behaviour of such alloys in carbon dioxide, and the present work is a continuation of previous investigations [3-5] of the oxidation of lower Fe/Ni alloys in carbon dioxide. The objects of the investigation were: (i) to study the kinetics of oxidation of an Fe/48 wt % Ni alloy in carbon dioxide at 700 to 1000° C; (ii) to examine the scale morphology as a function of time and temperature in order to determine which oxide or oxides were present; and (iii) to determine the form of internal oxidation in the alloy and investigate the redistribution of nickel during oxidation.

2. Experimental

Full details of the experimental techniques used have been given elsewhere [2,3]. The alloy used was Nilo 48 and was obtained from H. Wiggin & Co Ltd†, in the form of 0.25 in. diameter rod (1 in. = 2.5 cm). The cast analyses for this alloy were as follows (wt %): Ni, 48.7; C, 0.06; Si, 0.05; Cu, 0.04; Mn, 0.48; Mg, 0.027; Cr, 0.02; Al, 0.06; S, 0.011. Chemical analyses of the rod gave 48.4 wt % Ni and 0.43 wt % Mn. Specimens approximately 1.0 × 1.0 × 0.1 cm were milled for the oxidation studies, and a small hole was drilled in each specimen to allow suspension by a

*W. J. Tomlinson is now at the Department of Materials Science, Rugby College of Engineering Technology, Rugby, UK.
†Wiggin Street, Birmingham 16, UK.

fine platinum wire. Each specimen was polished to 4 O's emery paper, washed with acetone, and pickled in a sulphuric/nitric/hydrochloric acid mixture [6] for 2 min at 90° C. The kinetics of oxidation were determined using a quartz-spring thermobalance [7] which allowed weight changes to be measured to $\pm$ 0.0002 g. Syphon cylinder CO_2, containing $O_2 < 6$ ppm, $N_2 < 20$ ppm, and H_2O 70 ppm, was used, and the moisture content of the gas was reduced to < 10 ppm by passage through a $MgClO_4/P_2O_5$ drying train. Oxidation temperatures were controlled to within $\pm$ 2° C at 1000° C.

At the commencement of each run, the specimen was etched and washed with acetone, attached to the spring, and sealed into the thermobalance. The balance was then evacuated to a pressure of $< 10^{-5}$ mm Hg and brought to test-temperature. Carbon dioxide was then admitted to the balance and allowed to pass through it at $\sim$ 1 l/min. To terminate an experiment, the specimen was immediately winched out of the balance and was air-quenched. Three specimens were exposed under each condition (i.e. runs were carried out in triplicate).

Specimens for metallographic examination were mounted in a mixture of Araldite AY 103 with addition of Araldite hardener HY 951 and powdered calcite as a filler, using a vacuum impregnation technique previously described [8]. For electron probe microanalysis, specimens were mounted in a Thermosetting Silver Cement FSP 79 supplied by Johnson Matthey Ltd*. The iron, nickel, and manganese concentration profiles were measured in a Cambridge Mk II Microscan at several scanning speeds in the range 4 to 40 μm/min, and the peak values of nickel enrichment were checked by direct measurement of Bragg angles at these points. An accelerating voltage of 29 kV was used throughout.

The results have been corrected at appropriate places for paralysis time, background radiation, and, where relevant, fluorescence. The quantitative traces for iron and nickel shown in the various figures have been fully corrected at the points indicated and the complete curves have been adjusted accordingly. In all cases, several traces were obtained at various scanning speeds to ensure appropriate sensitivity of measurement and to allow elimination of statistical errors.

3. Results

The results will be presented in two sections dealing with kinetics and morphological studies respectively.

3.1. Kinetics of Oxidation

After a short period of irregular behaviour, the parabolic law was obeyed throughout the entire period of exposure, which varied from $\sim$ 1050 h at 713° C to 50 h at 1000° C (figs. 1 and 2). The

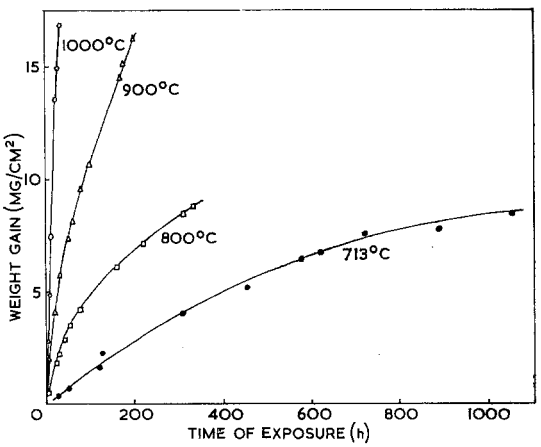

Figure 1 Oxidation of an Fe/48 wt % Ni alloy in CO_2 at 700 to 1000° C.

parabolic rate constants are presented in table I. It is clear that the rate of reaction increased with increasing temperature. The rate constants in table I were found to fit an Arrhenius function. The best straight line was calculated by the method of least mean squares. The activation energy was 47.8 $\pm$ 6.2 kcal/mole and the 95% confidence limit was evaluated by means of Student's t test.

TABLE I Parabolic rate constants for the oxidation of Nilo 48 in CO_2 (present work) and an Fe/41 wt % Ni alloy in O_2/N_2 mixtures [18].

Temperature	Parabolic rate constant (mg^2/cm^4 h)	
	Nilo 48 (CO_2)	Fe/41 wt % Ni (O_2/N_2)
1000	18.2	12.6 to 25.9
900	1.25	1.4 to 2.8
800	0.22	0.09
713	0.09	0.035

*Hatton Garden, London EC4.

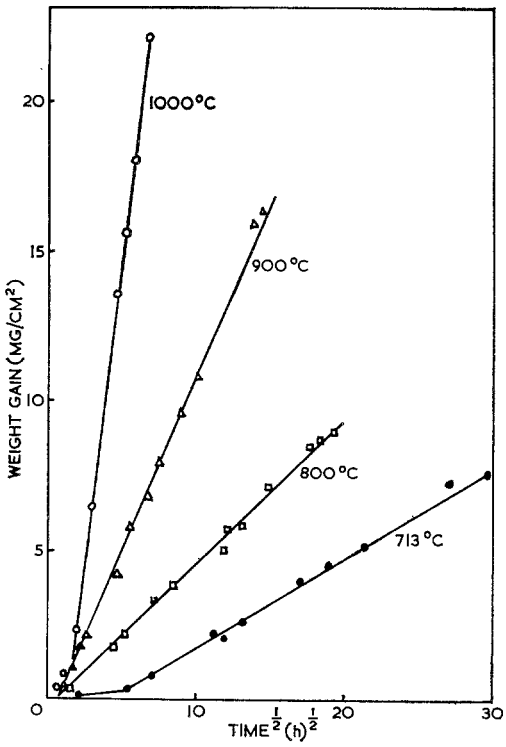

Figure 2 Parabolic scaling of an Fe/48 wt % Ni alloy in CO_2 at 700 to 1000° C.

TABLE II General features of scales formed at 1000° C.

Period of exposure	Wt gain (mg/cm²)	General features
10 min	1.0	Light-grey oxide containing 1 to 2 wt % Ni and 71 wt % total metal. Some penetration of oxide into alloy
30 min	2.0	7.5 to 12.5 μm thick scale with definite evidence of intergranular penetration (fig. 3a). Grain-boundary penetration in some regions to 25 μm depth and general precipitation of oxide particles ~1 μm diameter beneath scale. External scale contained 66 wt % Fe + 3.5 wt % Ni and maximum Ni concentration in the underlying alloy ~65 wt %
45 min	3.0	Regular scale/alloy interface and scale contained ~4 wt % Ni. Maximum Ni concentration in the underlying alloy 70 wt %
2 h	5.7	Less regular scale/metal interface with long oxide particles and a dispersion of small metal particles. Extensive oxide precipitation in grain bodies to a depth of 20 to 25 μm
4 h	7.2	General features similar to 2 h specimen. Progressive increase in internal oxide precipitation and depth of intergranular penetration
6 h	10.0	
8 h	11.1	
10 h	13.2	Evidence of larger metal particles isolated by oxide close to the metal/oxide interface. Grain-boundary oxide stringers, much thicker – possible evidence for second grain-boundary oxide (fig. 3c)

3.2. Morphological Studies

The scale and sub-scale structures were examined after various periods of exposure, mainly at 900 and 1000° C, using metallographic and electron probe microanalysis techniques.

3.2.1. Specimens Oxidised at 1000°C

The major features of film growth, composition, and nickel redistribution during the first 45 min of oxidation are summarised in table II and fig. 3a. It is clear that in this early period only one oxide phase was observed microscopically and, as oxidation proceeded, the nickel content of the oxide film increased to ~ 4 wt % and there was a rapid build-up in nickel concentration in the underlying metal to ~ 70 wt %. After 2 h exposure, the situation was more complex. Electron images (fig. 4a) showed the grain-boundary oxidation clearly, and X-ray images (figs. 4b and 4c) clearly indicated an iron-rich scale containing nickel and the nickel enrichment in the metal outlining grain boundaries. Slow scanning and point analyses allowed a detailed quantitative picture of the situation to be obtained (fig. 5). The maximum nickel enrichment was 75 wt % and the regions of intergranular oxide B′ and C′ (fig. 5a) corresponded to inverted peaks for nickel. The corresponding iron peaks were clear; absolute values of iron concentration at these points are inaccurate owing to the breadth of the boundary (2 μm).

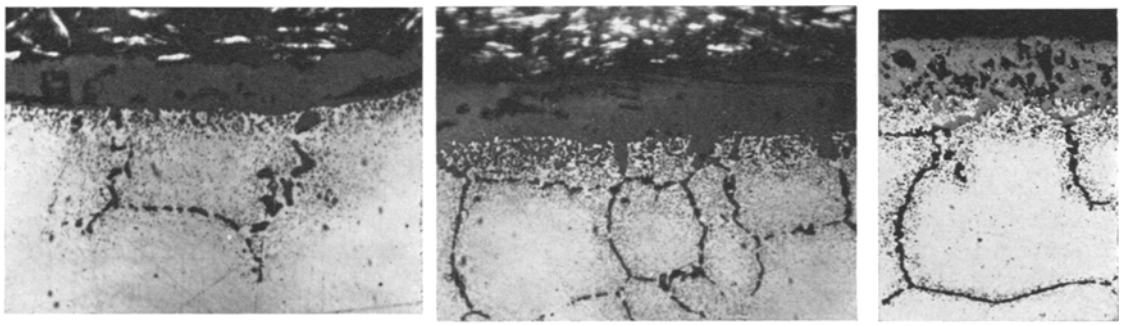

Figure 3 Cross-sections of alloy oxidised at 1000° C: (a) 30 min, etched (×550); (b) 2 h, etched (×275); (c) 10 h, etched (×122).

Observation of the nickel peak in the centre of the external scale was surprising, but appeared to be genuine since there was a corresponding decrease in the iron content at this point. The manganese concentration in the nickel-enriched metal grains was 0.6 wt %, whilst that in the external scale was 0.5 wt %. Thus there was no major segregation of manganese during oxidation.

After further periods of exposure, the general pattern of oxidation continued (table II) and detailed analyses were again carried out after 10 h exposure (figs. 4d-f and fig. 6). The overall pattern was more complex (fig. 6) but the analyses revealed a number of features. The general build-up of nickel had reached a level of 85 wt % and nickel-rich particles (C and D) were observed in the inner regions of the scale, which now contained 10 to 12 wt % Ni as compared with ~ 7 wt % in the external region of the scale. It should be noted that the region of oxide at E contains 7 wt % Ni and corresponds to the iron peak E in fig. 6b, which suggests that some localised regions of nickel-enriched oxide may be present. The presence of a second grain-boundary oxide could not be confirmed directly by electron probe analysis and again there was no segregation of manganese in the external scale. The clear evidence for grain-boundary oxide at points A and B should be noted. In this case, the oxide was probably thicker at point A, thus allowing a more accurate analysis of the vein to be obtained.

3.2.2. Specimens Oxidised at 900 and 800° C

A limited number of specimens were examined metallographically in order to confirm the morphological pattern observed at 1000° C and to examine the earlier stages in more detail. The results are presented in table III and figs. 7 and 8. It was clear from these results that internal precipitation of oxide occurred very early in the oxidation process and that intergranular penetration occurred in very localised areas initially, before becoming more general. After 10 h at 900° C, all of the features observed at 1000° C had been established. The 800° C specimen also fitted the morphological pattern at the other temperatures. Under all conditions, the external scale appears microscopically to be single phase.

3.2.3. Scale Growth Rates and Depth of Intergranular Oxide Penetration

The results of detailed examinations of the specimens were examined with a view to obtaining meaningful rates of growth of the external scale and the depth of intergranular penetration. There was considerable scatter in the results. At 900 and 1000° C, both the rate of overall growth of the scale and the rate of intergranular penetration were approximately parabolic functions.

4. Discussion

The presence of nickel in the oxide scale in this alloy is of considerable interest, since the scales on alloys containing $\leq$ 36 wt % Ni have consisted of wüstite and, in the early stages, of magnetite and wüstite [2-5]. Thus the critical nickel concentration in relation to its appearance in the oxide scale lies between 36 and 48 wt %, for oxidation in carbon dioxide. If we consider the thermodynamic possibilities (fig. 9), it is clear that, providing the CO/CO_2 pressure ratio $\leq 10^{-3}$, pure nickel and iron can oxidise to form NiO and Fe_3O_4 respectively. Whether or not nickel does appear in the scale under these conditions

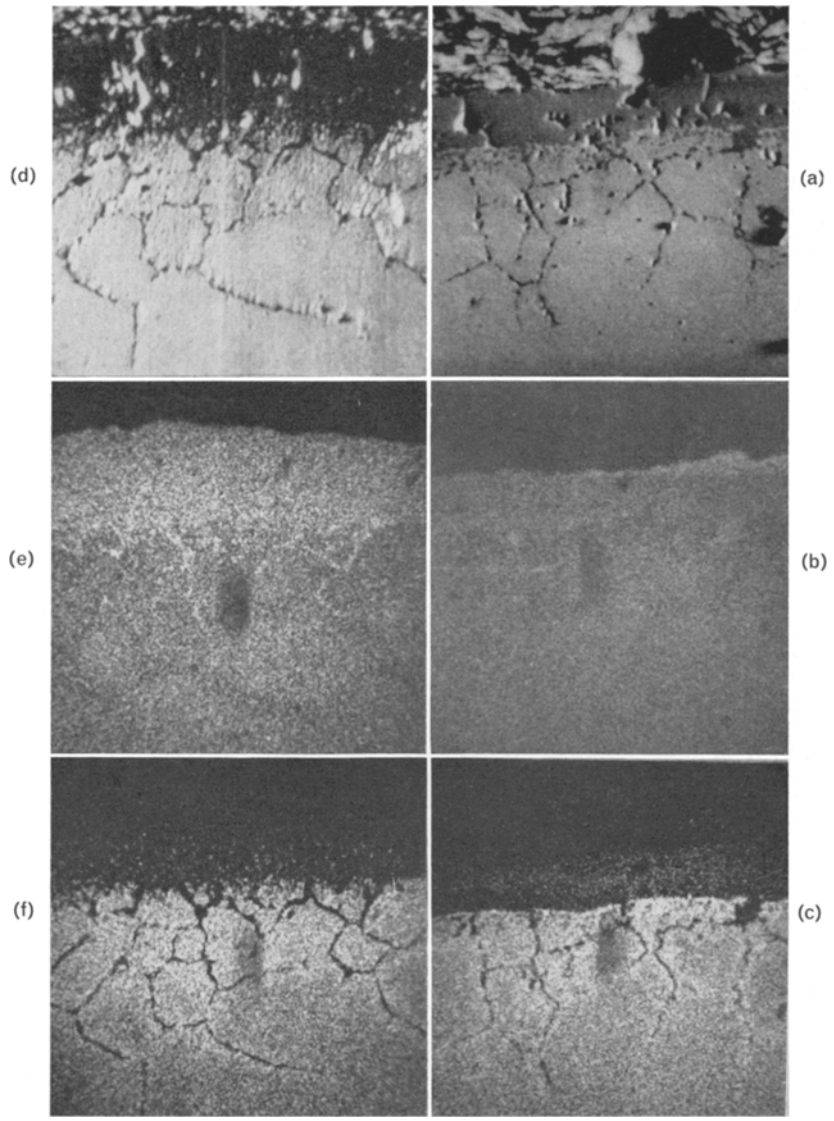

Figure 4 Electron and Fe and Ni Kα images on cross-sections of specimens oxidised at 1000° C: (a) electron image after 2 h (×250); (b) Fe Kα image after 2 h (×250); (c) Ni Kα image after 2 h (×250); (d) electron image after 10 h (×250); (e) Fe Kα image after 10 h (×142); (f) Ni Kα image after 10 h (×142). (The X-ray images are prints – light for high concentrations.) (a, b, c, × 237; d, e, f, × 135.)

depends also upon the activity of nickel in the alloy. Since the Fe/Ni system is an ideal solid-solution system [9,10], the activities of iron and nickel in this alloy will be ~ 0.5. This will decrease the free energy of formation of NiO in the reaction Ni (alloy) $+ \frac{1}{2}O_2 \rightarrow$ NiO and this will be of greatest importance at low temperatures (fig. 9), where oxidation of nickel is more difficult. The experimental conditions in the present investigation (high flow rate of carbon-dioxide) are such that the CO/CO_2 pressure ratio $< 10^{-3}$, and hence the presence of nickel in the scales at 1000° C is not unexpected. Furthermore, the enrichment of nickel in the underlying alloy at this temperature is rapid, the nickel content being 65 wt % after only 30 min of oxidation. Thus the absence of FeO in the scales and outer grain-boundary oxide is not surprising, since,

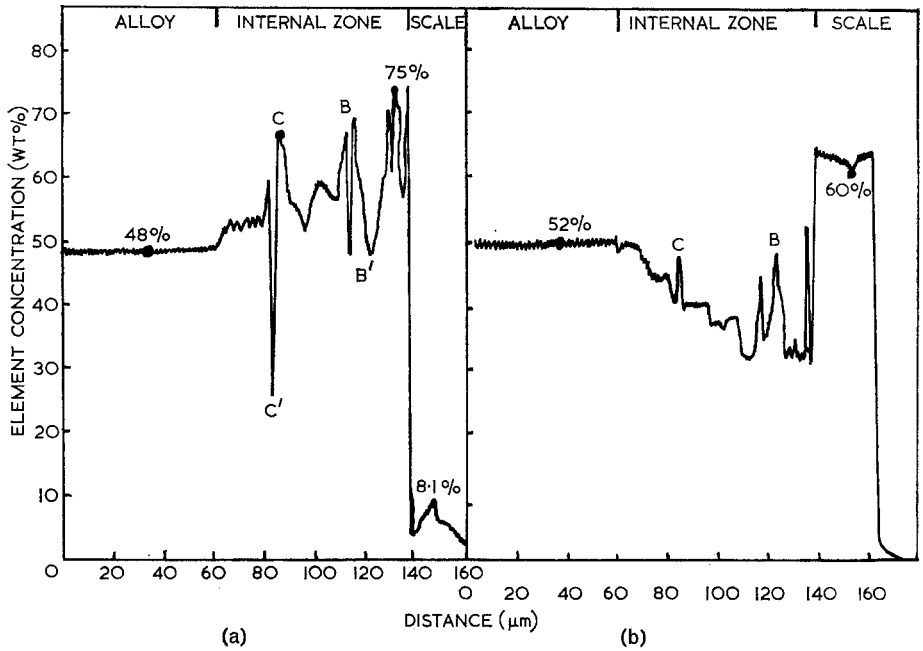

Figure 5 Ni (a) and Fe (b) concentration profiles across specimens oxidised for 2 h at 1000° C.

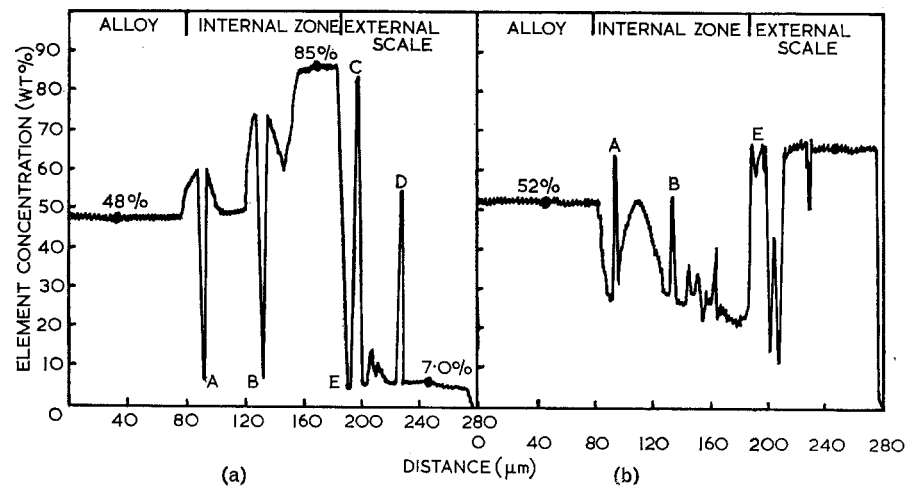

Figure 6 Ni (a) and Fe (b) concentration profiles across specimens oxidised for 10 h at 1000° C.

under equilibrium conditions, spinel [11] would be expected in contact with alloy containing $\geq$ 55 to 60 wt % Ni. The intergranular penetration of oxide in this alloy is not unexpected, in view of similar observations for an Fe/36 wt % Ni alloy [4], and it is clear, from present studies and those of other workers in oxygen [12], that the higher nickel alloys are more prone to this type of attack. However, it is also clear from figs. 3, 7, and 8 that there is considerable precipitation of small oxide particles within the grain bodies close to the metal/oxide interface and in the region of the grain boundaries at greater depths within the alloy.

The composition of the nickel ferrite phase is of considerable interest, since there are clearly gradients with respect to nickel concentration. It should be noted that solid solutions of $NiFe_2O_4$ in Fe_3O_4 (i.e. $Ni_xFe_{3-x}O_4$, where $x \leq 0.5$) are almost ideal solid solutions [13]. Further work

TABLE III Metallographic features of scales formed at 900 and 800° C.

Temperature of exposure (° C)	Period of exposure	Wt gain (mg/cm²)	General features
900	30 min	0.8	2 to 5 μm thick oxide appeared to be single phase. Localised internal oxide precipitation to a depth of ≤10 μm (fig. 7a)
900	3 h	1.4	Similar pattern (fig. 7b), scale 5 to 8 μm thick. Localised internal precipitation to 25 μm depth. Intergranular oxidation localised
900	10 h	3.8	(fig. 7c) Grain-boundary oxidation now fully established and locally up to 50 μm in depth. Zone of extensive internal oxide precipitation 12.5 μm deep immediately underlying external scale
800	25 h	2.3	(fig. 8) Apparently single-phase oxide 7 to 8 μm thick. Grain-boundary oxidation localised to few areas. Precipitation of internal oxide particles to 5 to 8 μm depth

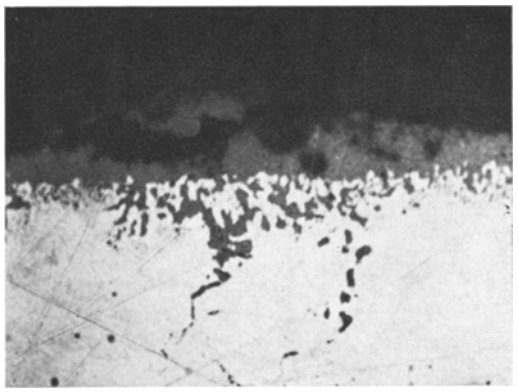

Figure 8 Cross-section of alloy oxidised for 25 h at 800° C, etched (×656).

on the nucleation stage is necessary in order to decide whether direct nucleation of the spinel phase occurs or whether both iron oxide(s) and NiO nucleate, the spinel being formed by surface and interdiffusion processes. Foley, Guare, and Schmidt [14] have reported the presence of $Ni_xFe_{3-x}O_4$ and Fe_2O_3 in the early stages of oxidation of an Fe/41 wt % Ni alloy in air. The results at 1000° C, however, indicate that nickel is present in the scale in the early stages of oxidation and, after 10 min, the oxide corresponds to $Ni_{0.06}Fe_{2.94}O_4$. As oxidation proceeds, there is considerable enrichment of the scale in nickel, and the spinel composition becomes close to $Ni_{0.4}Fe_{2.6}O_4$ near the metal/oxide interface. Kennedy, Calvert, and Cohen [12] reported a spinel phase, $Ni_{0.43}Fe_{2.57}O_4$, on an Fe/25 wt % Ni alloy oxidised at 800° C; whereas Yearian, Boren, and Warr [15] obtained $Ni_{0.05}Fe_{2.95}O_4$ and $Fe_{0.53}Fe_{2.47}O_4$ on a similar alloy in air saturated with water vapour, at 871 and 982° C. A variety of spinel compositions was obtained at

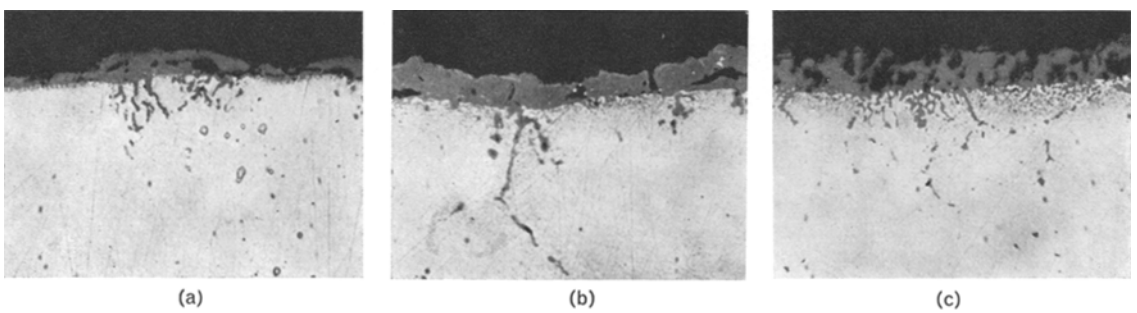

Figure 7 Cross-sections of alloy oxidised at 900° C: (a) 30 min, etched (×470); (b) 3 h, etched (×470); (c) 10 h, etched (×235).

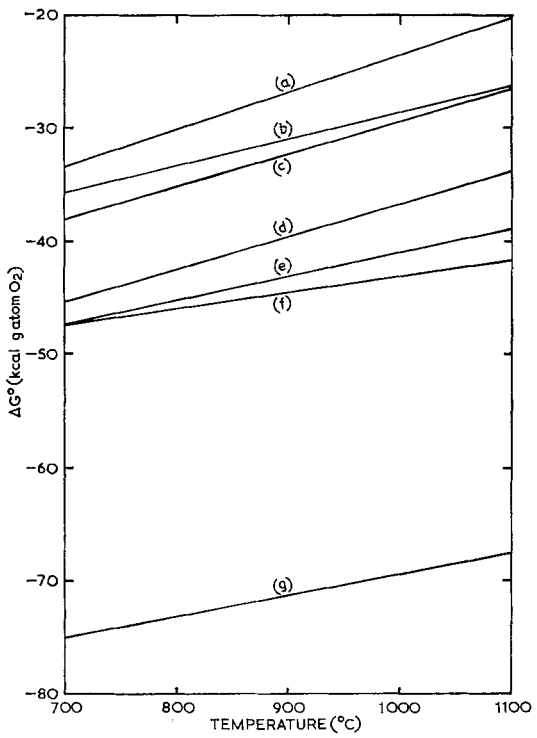

Figure 9 Standard free energies of formation of metal oxides and carbon dioxide [19]: (a) $CO + \frac{1}{2}O_2 \rightarrow CO_2$, $p_{CO}/p_{CO_2} = 10^{-3}$; (b) $Ni + \frac{1}{2}O_2 \rightarrow NiO$; (c) $CO + \frac{1}{2}O_2 \rightarrow CO_2$, $p_{CO}/p_{CO_2} = 10^{-2}$; (d) $3FeO + \frac{1}{2}O_2 \rightarrow Fe_3O_4$; (e) $CO + \frac{1}{2}O_2 \rightarrow CO_2$, $p_{CO}/p_{CO_2} = 1$; (f) $Fe + \frac{1}{2}O_2 \rightarrow FeO$; (g) $Mn + \frac{1}{2}O_2 \rightarrow MnO$.

1093° C with the most nickel-rich spinel in the outer regions of the scale. This is an unexpected finding and is not in agreement with the present results or those of Foley [16].

In the present work, there was no evidence for major segregation of manganese in the nickel ferrite phase as the maximum manganese concentration in the scale was 0.5 wt % and that in the intergranular oxide 0.6 wt %. Thus, although on thermodynamic grounds (fig. 9) oxidation of manganese would be expected, its activity is low. The presence of chromium in Hastelloy X (in wt %: 47.6, Ni; 21, Cr; 18.8, Fe; 8.9, Mo; 1.8, Co; 0.47, Mn) with preferential oxidation of this element [17], however, also appears to promote formation of $MnCr_2O_4$ during oxidation of this alloy in CO_2 at 1000° C. However, the total amount of oxidation is much less, which probably also facilitates concentration of this element in the scale, as also occurs with some Fe/Cr/Ni alloys [15].

In the present study, Nilo 48 behaved in a parabolic manner and hence it is reasonable to assume that oxidation proceeds under diffusion control. Since the only oxide present is $Ni_xFe_{3-x}O_4$, it also is reasonable to assume that the rate-controlling process is diffusion of iron through this phase. Since it has been suggested [16,18] that diffusion of iron in the spinel phase is the rate-controlling process during the oxidation of similar alloys in oxygen, it is of interest to compare the rate constants obtained in the present studies with data for O_2/N_2 mixtures (table I). It can be seen that the rates of oxidation of an Fe/41 wt % Ni alloy at 900 to 1000° C are similar to those of Nilo 48 in carbon dioxide. At lower temperatures, however, the rate of oxidation of Nilo 48 is faster than that of the Fe/41 wt % Ni alloy and this is most probably due to a decrease in the nickel content of the oxide phase at these lower temperatures, since (fig. 9) oxidation of nickel is more difficult at these temperatures. The agreement of the results with Foley's data is remarkable, since his exposure times were only 60 min. Clearly, more information concerning the relationship between the diffusion coefficient for iron and the nickel concentration in oxides of the type $Ni_xFe_{3-x}O_4$ is required. The activation energy (47.8 $\pm$ 6 kcal/mole) is also in reasonable agreement with Foley's value [16,18] of 41 kcal/mole. It should however be noted that, in oxygen or O_2/N_2 mixtures, an outer layer of Fe_2O_3 is also present. The fact that the oxidation rates of the two alloys are similar, and have similar activation energies, indicates that diffusion of iron through the spinel phase is the rate-controlling process in both cases.

Acknowledgements

The authors wish to thank Professor T. K. Ross for the provision of research facilities and the Science Research Council for the provision of the microanalyser. One of us (W.J.T.) also wishes to thank the Council for the award of a research studentship.

References

1. R. T. FOLEY, *J. Electrochem. Soc.* **109** (1962) 1202.
2. W. J. TOMLINSON, Ph.D. thesis, University of Manchester (1965).
3. I. A. MENZIES and W. J. TOMLINSON, *J. Iron & Steel Inst.* **204** (1966) 1239.
4. *Idem, British Corrosion J.* (1967), in press.
5. *Idem*, in preparation.
6. R. T. FOLEY *et al*, *J. Electrochem. Soc.* **102** (1955) 440.

7. I. A. MENZIES and K. N. STRAFFORD, *Corros. Sci.* **3** (1963) 193.
8. I. A. MENZIES and D. MORTIMER, *ibid* **6** (1966) 517.
9. O. KUBASCHEWSKI and O. VON GOLDBECK, *Trans. Far. Soc.* **45** (1949) 948.
10. R. ORIANI, *Acta Met.* **1** (1953) 448.
11. M. J. BRABERS and C. E. BIRCHENALL, *Corrosion* **14** (1958) 179t.
12. S. W. KENNEDY, L. D. CALVERT, and M. COHEN, *Trans. AIME* **215** (1959) 64.
13. I. V. GORDEEV and YU. D. TRETYAKOV, *Vestn. Mosk. Univ.* Ser. 11, Khim 18, No. 2 (1963) 32.
14. R. T. FOLEY, C. J. GUARE, and H. R. SCHMIDT, *J. Electrochem. Soc.* **104** (1957) 413.
15. H. J. YEARIAN, H. E. BOREN, and W. E. WARR, *Corrosion* **12** (1956) 561t.
16. R. T. FOLEY, *J. Electrochem. Soc.* **109** (1962) 1202.
17. J. M. FRANCIS, J. A. JUTSON, and J. H. BUDDERY, *J. Matls. Sci.* **2** (1967) 78.
18. R. T. FOLEY and C. J. GUARE, *J. Electrochem. Soc.* **106** (1959) 936.
19. C. E. WICKS and F. E. BLOCK, "Thermodynamic Properties of 63 Elements – their Oxides, Halides, Nitrides and Carbides", *US Bur. Mines Bull.* **605** (1963).